Nuclear Instruments and Methods in Physics Research B13 (1986) 443–448
North-Holland, Amsterdam

COMPUTER CALCULATIONS OF SECONDARY PARTICLE EMISSION NEAR THE CURIE POINT OF NICKEL

V.A. ELTEKOV, V.N. SAMOYLOV and V.E. YURASOVA

Department of Physics, Moscow State University, Moscow 117234, USSR

H.A. MOTAWEH

Department of Physics, Faculty of Science, Tanta University, Tanta, Egypt

The method of computer simulation is used to study the 200 eV Ar^+ ion interactions with (001) Ni single crystal face in ferromagnetic and paramagnetic states. The integral yields and the spatial and energy distributions of the sputtered and transmitted atoms and of reflected ions have been obtained. The differences in the data obtained for ferro and paramagnetic nickel are discussed.

1. Introduction

The study of the secondary atomic particle emission and ion reflection from solids under ion bombardment in the temperature interval including the points of phase transitions (for example, polymorphic and magnetic) is a new field of engineering material science and the physics of atomic particle interactions with solids [1–6].

The effect of polymorphic transformation on the processes of atomic particle emission is contingent, to a great extent, on such geometric factors as the crystal lattice rearrangement and the "transparency" variations. The main role in the magnetic phase transitions is played by the exchange interaction whose value varies because of reorientation of the magnetic moments of atoms. Therefore, the changes of the secondary atomic particle emission under magnetic transitions may carry information about the details of electron structure and interactions of atoms in magnetics. The study of the secondary emission under such conditions is of not only scientific, but also applied interest. For example, an ever growing number of magnetic substances are being used as engineering materials in a broad range of temperatures and under the conditions of intensive irradiation. Besides that, the knowledge of the regularities defining the effect of phase transitions in metals on the ion bombardment-induced particle emission is of great importance for developing surface analysis methods.

The effect of magnetic f–p phase transitions on sputtering and reflection of ions from Ni single crystals and polycrystals under ion bombardment has been studied in several experiments (see refs. [1, 3–6]). The changes observed experimentally were explained in ref. [2] by the fact that a spin–spin term affecting the sputtering process appears in the two-atomic interaction potential for the ferromagnetic state of Ni.

The single-crystal sputtering was examined in ref. [2] by studying separately the changes of the focuson and cascade (in amorphous media) contributions to sputtering under the f–p transition. The joint analytical study of the two mechanisms of the changes in the single-crystal sputtering is impossible because the set of equations involved is too tedious. Therefore, the role of direct computer simulation of the process becomes important.

On the other hand, the effect of magnetic phase transition on the integral yield of reflected ions and on ion transmission was not studied theoretically. The relationship between the sputtering and scattering of ions under magnetic phase transitions was not analyzed either. In this work, an attempt is made to solve the problems by calculating a complex of the processes which accompany the ion bombardment of single crystal (reflection and transmission of ions, propagation of collision cascades and sputtering) in terms of the many-particle interaction model. We shall examine the case of normal incidence of 200 eV Ar^+ ions onto the (001) Ni face.

2. Calculational model

Use was made of the many-particle interaction model described in ref. [7]. The 200 eV Ar^+ ions bombard a surface element of a crystallite of 411 Ni atoms arranged in six layers with the (001) face on its surface.

The model allowed for the interactions of all atoms with moving ions and with each other through the

0168-583X/86/$03.50

paired central forces. The Ar^+–Ni and Ni–Ni interaction potential was assumed to consist of two parts [7]. At distances $r < 0.392$ Å, the inverse-square potential $V(r) = C/r^2$ with the parameters $C = 3.05\ Z_1 Z_2 (Z_1^{1/2} + Z_2^{1/2})^{-2/3}$, where Z_1 and Z_2 are nuclear charges of the interacting atoms was used. At distances $0.392\ \text{Å} \ll r < r_0$, the Born–Mayer potential with the parameters $A = C[e/(2b)]^2$, where $b = 0.196$ Å, $e = 2.7182\ldots$, was used. At $r \geq r_0$ the potential $V(r)$ is zero, $r_0 = 4$ Å.

The use of the repulsion potentials instead of the repulsion–attraction potentials has made it possible to estimate the individual contributions of the cascade variation and the binding energy variation on the surface to the change of the sputtering yield. The binding energy on the surface (in the assumption of the spherical potential barrier) was chosen either to equal the sublimation energy for Ni (4.435 eV [8]) or to be determined by static approximation [9]. The use of the repulsion potentials made if necessary to control the stability of the crystal. The analysis has shown that, within the process evolution time (usually not longer than 200–500 fs), the changes in the crystallite were minor and did not introduce any error to the recorded parameters.

The nickel ferromagnetism was only included by adding the spin–spin term $-\Delta V_f(r) = A_1 e^{-b_1 r^2}$ ($A_1 = 5.16$ eV, $b_1 = 0.8112$ Å^{-2}) to the interaction potential of two Ni atoms in the f-state. The ion–atom potential was assumed not to vary under the f–p transition.

The model also made allowance for the thermal vibrations of lattice atoms. They were assumed to be uncorrelated and symmetric with respect to the lattice sites and were calculated in the same way as in ref. [7] using $T_D = 470$ K for Ni. The equations of motion were integrated using the "mean force" method proposed in ref. [10]. The impact points totalled 100. We limited ourselves to this number because in ref. [7] it was shown that the use of a greater number of impact points does not significantly change the calculated results.

In case of the f- and p-states, the impact points of 100 ions were the same which made it possible to effectively use the correlation of the results obtained and reduced the error of the difference in the values obtained for the f- and p-states.

In the simulation, the energies and motion directions of all the particles ejected from the crystal were calculated for each ion incidence event. The processing of the data thus obtained made it possible to construct the spatial and energy distributions of sputtered and transmitted atoms and reflected ions (see figs. 1–4). Besides that, the sputtering yield $S_\uparrow$, the yield of the transmitted atoms $S_\downarrow$, the yield of atoms sputtered through the lateral faces of block $S_{\rightarrow}$ and the reflection factor $R_\uparrow$ were calculated. The ion–crystal interactions were only calculated for two states (para- and ferromagnetic) of the target disregarding the magnetization fluctuations which are largest near the Curie point. Thus the results obtained in this work may be compared with the experimental data for temperatures far from the Curie point.

3. Results and discussion

3.1. Sputtering yields

The f-state Ni sputtering yield was calculated here at binding energy $E_b = 4.435$ eV in terms of the model without thermal vibrations and proved to be $S_{\uparrow f} \sim 1.6$ atoms/ion. As compared with the experimental data this value is overestimated. The overestimation may be due to different reasons. One of them is the use of spherical (instead of planar) barrier on the surface. (According to the estimates [11], the use of a planar barrier may decrease the value of $S_\uparrow$ by a factor of 3). The resultant disagreement between the calculated and experimental values of $S_\uparrow$ is not, nevertheless, essential when studying the relative variations of the sputtering yield under f–p transition. Under the transition the sputtering yield increased up to $S_{\uparrow p} \sim 1.9$ atoms/ion, i.e. by ~17%. The yield of transmitted atoms (which was also calculated using the spherical surface potential barrier with $E_b = 4.435$ eV) increased under the f–p transition from $S_{\downarrow f} \sim 3.6$ to $S_{\downarrow p} \sim 3.8$ atoms/ion, i.e. by ~8%. The variations exceed those obtained by analytical estimations [2].

After introducing the thermal vibrations corresponding to $T = 630$ K, i.e. the temperature of magnetic phase transition in Ni, the sputtering yields varied to reach $S_{\uparrow f} \sim 1.9$ atoms/ion and $S_{\uparrow p} \sim 2.3$ atoms/ion, while the yields of forward-sputtered atoms reached $S_{\downarrow f} \sim 3.4$ atoms/ion and $S_{\downarrow p} \sim 3.8$ atoms/ion.

Thus, the inclusion of thermal vibrations of atoms resulted in an increase of $S_{\uparrow f}$ by ~18% compared with the static lattice. In the case of $S_{\uparrow p}$, the increase was ~22%. The increases are probably due to the fact that, on introducing the thermal vibrations, the collision cascades develop nearer to the surface and, therefore the energy lost by an ion in a near-surface layer increases, therefore the sputtering yield also increases.

The introduction of thermal vibrations did not, however, give rise to any increase in the yield of transmitted atoms, namely, $S_{\downarrow p}$ does not vary within statistical errors and $S_{\downarrow f}$ even decreases because, probably, the cascade develops nearer to the surface with a more effective defocusing of correlated collision chains and a stronger deceleration of ions in the upper layers.

In terms of the model with thermal vibrations (E_b = constant = 4.435 eV, $T = 630$ K), the sputtering yield under the f–p transition increased by ~21%, and the yield of transmitted atoms by ~13%. Thus, the introduction of thermal vibrations enhances the effect of

the change of the yields of sputtered and transmitted atoms when changing the magnetic state of the substance.

The data presented above were obtained by calculating the Ni sputtering yield under magnetic phase transition due only to the change of the collision cascade. The binding energy on the surface was assumed to be constant and equal to the experimental value of sublimation energy. However, the binding energy of an atom on the surface under f–p transition also suffers variations. The variation of the binding energy E_b of an atom in a site on the (001)Ni face surface was calculated in ref. [9] for the static approximation. In the f-state, E_b proved to be ~5% as high as in the p-state. The inclusion of the binding energy variation under f–p transition results in a ~27% increase of $S_\uparrow$ under magnetic phase transition (allowing for thermal vibrations). This value agrees better with the results of the experiment with Ni polycrystal sputtering under 200 eV Ar^+ ion bombardment [4].

The spatial and energy distributions of the sputtered and transmitted atoms and the atoms sputtered to the ⟨110⟩ spot through the lateral faces of the crystallite were also obtained.

3.2. Spatial distributions of sputtered particles

Fig. 1. presents the spatial distributions of the sputtered and forward-sputtered atoms for Ni in the p-state. It is seen that in both cases the sputtered particles are ejected predominantly to four spots corresponding to close-packed directions of the ⟨110⟩ type while the transmitted particles are ejected to the spot ⟨001⟩ and four spots ⟨110⟩. Because of the blocking effect, the ⟨110⟩ spots in the spatial distributions of the sputtered and transmitted atoms are shifted towards a normal to the surface, just as in the experiment (cf [12, 13]). The distributions for the f-states near the ⟨110⟩ spots are somewhat narrower than in case of the p-state for both backsputtered and transmitted atoms. The spatial distributions of the atoms ejected through the lateral faces of the crystal displayed maxima in four ⟨110⟩ directions lying in the plane of the surface and perpendicular to the primary ion beam incidence directions. There maxima are probably produced by the atoms ejected by the mechanism of perpendicular focusing. (The favourable conditions for the focusing of the momentum of moving atoms are created in the close-packed directions perpendicular to the ion beam incidence direction). We have found that the number of atoms sputtered to four ⟨110⟩ spots through the lateral faces of the crystallite ($S_{\rightarrow}$) increases under the f–p transition from $S_{\rightarrow_f} \sim 2.6$ atoms/ion to $S_{\rightarrow_p} \sim 2.7$ atoms/ion, i.e. by 5% (in terms of the model without thermal vibrations with E_b = constant = 4.435 eV).

Because of the inclusion of the thermal vibrations corresponding to $T = 630$ K, the yield of atoms to the ⟨110⟩ spots through the lateral faces of the crystallite $S_{\rightarrow}$ changes to $S_{\rightarrow_f} \sim 2.2$ atoms/ion and $S_{\rightarrow_p} \sim 2.4$ atoms/ion (at E_b = constant = 4.435 eV). Thus, the inclusion of thermal vibrations of atoms results in a ~14% decrease of $S_{\rightarrow_f}$ compared with the data obtained in terms of the static lattice model. The

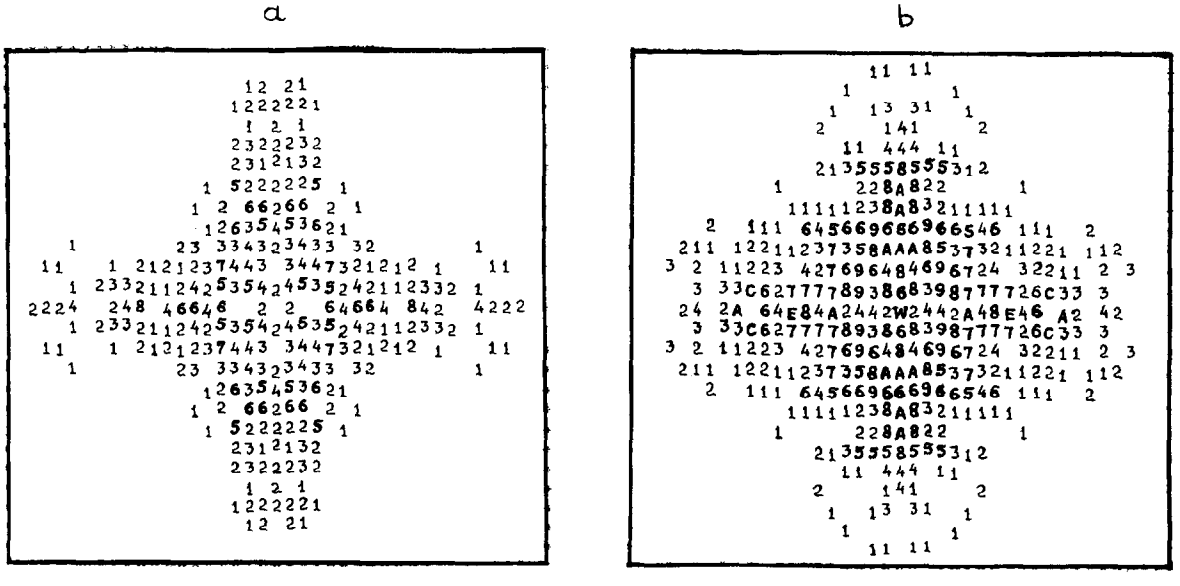

Fig. 1. Spatial distributions of sputtered atoms (a) and transmitted atoms (b) for paramagnetic Ni in the model without thermal vibrations (E_b = 4.435 eV) for the particles emitted at angles from 0 to ±45° from the normal to the surface. The number of atoms emitted to a certain point of the plane collector is given by figures from 1 to 9 and then by letters. The centers of both pictures correspond to the [001] directions.

decrease in $S_{\rightarrow p}$ proved to be ~13%. This trend is probably due to the fact that the inclusion of thermal vibrations decreases the contribution of focusons to $S_{\rightarrow}$.

The number of atoms sputtered to four ⟨110⟩ spots through the lateral faces of the crystallite, $S_{\rightarrow}$ under the f–p transition increased by ~6% in the model with thermal vibrations (E_b = constant = 4.435 eV, T = 630 K). Thus, the introduction of thermal vibrations will somewhat enhance the effect of the changes in the yield $S_{\rightarrow}$ as a result of a change of the magnetic state of the substance.

3.3. Energy distribution of sputtered atoms

Fig. 2 shows the energy spectra of the sputtered atoms, the transmitted atoms, and the atoms sputtered to the lateral ⟨110⟩ spots through the lateral crystallite faces for p-Ni (in the model without thermal vibrations at E_b = 4.435 eV).The atoms with $E < 0.2$ eV are observed in the sputtered particle spectrum. The high-energy side of the spectrum exhibits a peak in the 16–34 eV range. A similar high-energy peak was obtained in the calculations [7]. It can be seen that the peak in the spectrum of the atoms sputtered through the lateral faces is somewhat shifted to higher energies compared with the peaks of the rest spectra. The shift is probably due to the features of the momentum focusing mechanisms in the directions perpendicular to the primary beam incidence direction (see ref. [12]). What is quite obvious is the increase of the maximum energy of the ejected atoms when changing over from the sputtered particle spectrum to the spectrum of the particles ejected through the lateral faces and to the distribution of the transmitted atoms (the rise from 34 eV to ~44 eV and ~120 eV).

The change of the target magnetic state fails to give rise to qualitative changes in the spectrum of sputtered atoms. Fig. 3 shows the energy spectra of the transmitted atoms and of the atoms ejected through the lateral faces for Ni in the f- and p- states. In case of the f-p transition, the particle number increase is observed in the medium-energy range (from ~1 eV to ~10 eV) of the spectrum of the transmitted atoms and in the low-energy range (from ~0.3 eV to ~1 eV) of the spectrum of the atoms ejected through lateral faces. As should be expected, the high-energy part of the spectra ($E \geq 34$ eV) proved to be least sensitive to the target magnetic state.

Fig. 4 shows the energy spectra of the transmitted atoms for p-Ni in the models without thermal vibrations and with the vibrations corresponding to T = 630 K, T_D = 470 K (E_b = constant = 4.435 eV). Despite the fact that the values of $S_{\downarrow p}$ in the models without thermal vibrations and for T = 630 K are almost the same, the energy spectra of the transmitted atoms are very different. In the model with thermal vibrations, the peak of the spectrum and of its high-energy part is shifted by ~2–3 eV toward higher energies. This effect may probably be attributed to the fact that, as a result

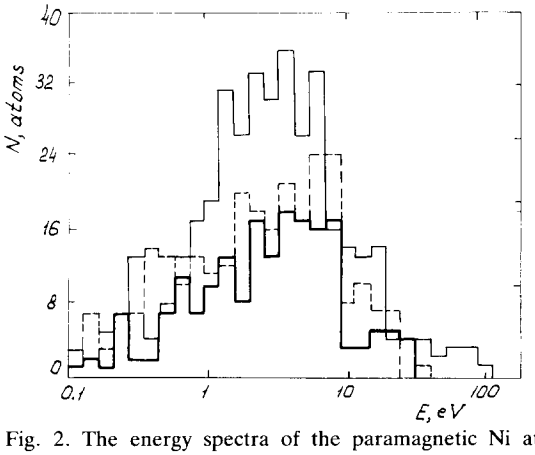

Fig. 2. The energy spectra of the paramagnetic Ni atoms in the model without thermal vibrations: ——, sputtering; ----, sputtering through lateral faces; ——, transmission sputtering.

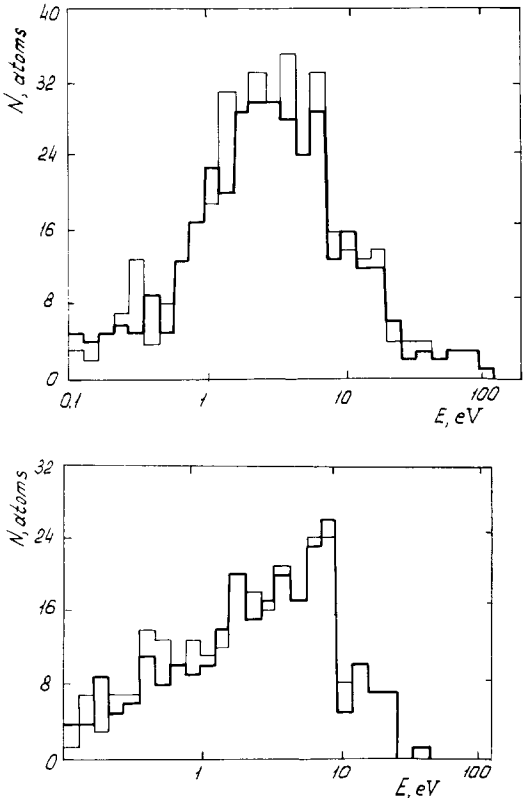

Fig. 3. The energy spectra of the transmitted atoms (a) and the atoms sputtered through lateral faces (b) of ferromagnetic (——) and paramagnetic (—-—)Ni in the model without thermal vibrations.

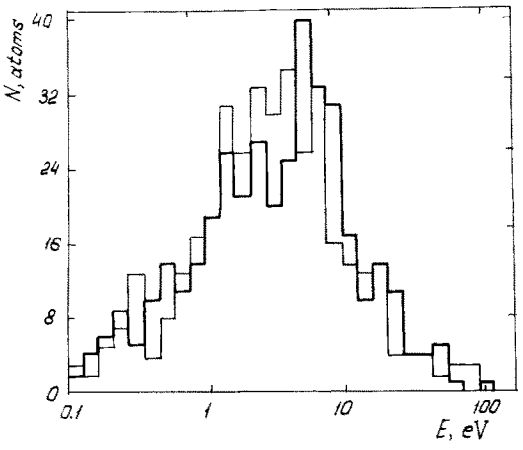

Fig. 4. The energy spectra of the transmitted Ni atoms at $T = 630$ K (——) and in the absence of thermal vibrations (——) in the paramagnetic state.

of the inclusion of thermal vibrations, the probability for the ions incident along the ⟨001⟩ open channel ($E_0 = 200$ eV) to transfer a larger fraction of their energy to the atoms in the nearly head-on collisions increases, thereby raising the energy of the transmitted atoms. The stronger defocusing of the collisions and the increased energy loss resulting from the inclusion of thermal vibrations will probably lead to an increase in the fraction of low-energy particles (with $E \leqslant 0.5$ eV) in the sputtered particle spectrum.

3.4. *Scattering of ions*

We have also calculated the integral reflection factor of ions, $R_\uparrow$ for the f- and p-states of Ni disregarding the charge state of the reflected ions in terms of the model without thermal vibrations. The value of $R_\uparrow$ proved to rise from 0.7 to 0.8 under the f–p transition. The rise is probably due to the fact that the atom–atom potential is more rigid in the p-state (the addition $\Delta V_f(r)$ is negative at any distance r), as a result of which the energy E transferred from ion to atom decreases. Besides that, the ion–atom interaction cross section, which is smaller in the p-state, changes under the f–p transition. It is the combined effect of the two factors for multiple reflection and simultaneous interaction of one ion with several atoms that results probably in the observed increase of $r_\uparrow$ under the f–p transition.

The model without thermal vibrations was also used to calculate the probability of Ar^+ ions implanted in the six-layer crystallite. This probability proved to decrease under the f–p transition from 0.27 to 0.16, i.e. by ~41%. If this result is confirmed experimentally, it may be used in the ion doping technique, namely, the number of low-energy ions implanted to the ferromagnetic surface can be significantly changed by varying the temperature of the ferromagnetic.

According to the experimental data [5, 6], the differential factor of ion reflection from a Ni crystal surface decreases under the f–p transition. However, the experiments [5, 6] allowed only for the charged fraction of the reflected ion beam. Comparison of the experimental data [5, 6] with the result of the present work suggests that the change of the degree of neutralization of the ions reflected from the surface under magnetic transition plays a more important role than the change of the interaction potential of atomic particles.

4. Conclusions

The model of many-particle interactions was used to study the ion reflection and the sputtering and transmission of atoms in a single computer simulation experiment. The case of the normal 200 eV Ar^+ ion incidence onto the (001)Ni face in ferro- and paramagnetic states was examined.

(1) A ~27% increase of the sputtering yield under the f–p transition has been found. The variation of the collision cascade indicated a greater change of the Ni single crystal sputtering yield (~21%) compared with the contribution of the binding energy variation (~5%). The relative difference in the sputtering yields in the f- and p-states has been shown to rise with an increase in the mean multiplicity of the collisions which give rise to the particle sputtering. The relative difference in the sputtering yields also rises when thermal vibrations are included in the model.

(2) The yield of transmitted atoms has been shown to increase by ~13% under the f–p transition. The difference in the yields of transmitted atoms indicated an increase if allowance was made for thermal vibrations.

(3) The integral factor of Ar^+ ion reflection (disregarding the charge state) from the (001)Ni face has been found to increase by ~11% under the f–p transition.

(4) The integral reflection factor indicated to be sensitive to the changes of not only ion–atom but also atom–atom potentials. This is due to the fact that the 200 eV ions were scattered by the bound atoms rather than by the free atoms, as assumed in the binary collision model.

(5) The low-energy atom implantation to the near-surface Ni single crystal layer has been shown to decrease significantly (by ~40%) under the f–p transition.

The results obtained in this work and bearing on the variations of the ion sputtering and reflection under the f–p transition must be allowed for when analyzing the

particle balance in the case of ion bombardment of the surfaces of engineering materials. Indeed, it was found in ref. [14], for example, that, when irradiated by ions, the non-ferromagnetic austenite chrome–manganic steel, which is a promising material for the manufacture of the first wall of fusion reactors, became ferromagnetic down to a ~300 Å depth from the surface. At the same time, it is known that thermonuclear reactors are expected to operate under thermocycling conditions and that the wall temperature will probably vary from 200°C to 600°C (see, for example, ref. [15]). Therefore, the changes of the sputtering yield and reflection factor of ions under the f–p transition in ferromagnetics must be allowed for when calculating the particle and energy balance in the case of the ion bombardment of the first wall of a thermonuclear reactor. The inclusion of these changes is also of importance in other applications; for example, when analyzing the surface composition by means of ion beams.

The authors are indebted to Dr M.V. Kuvakin for informative discussions of the results.

References

[1] V.E. Yurasova, V.S. Chernysh, M.V. Kuvakin and L.B. Shelyakin, Pis'ma ZhETF 21 (1975) 197.

[2] M.V. Kuvakin, Thesis, Moscow State University, Moscow (1979).

[3] V.E. Yurasova, Vacuum 33 (1983) 565.

[4] L.B. Shelyakin, T.P. Martynenko, A. Bischoff, V.E. Yurasova and R. Scharschmidt, Surface N6 (1983) 65 (in Russian).

[5] I.N. Evdokimov, Pis'ma ZhETF 6 (1980) 186.

[6] M.V. Kuvakin, V.A. Abramenko and V.E. Yurasova in: Diagnostics of Surface by Ion Beams, Abstracts of Repts at All-Union Seminar of Young Scientists, Uzhgorod (1985) p. 239.

[7] V.A. Eltekov, V.N. Samoylov and V.E. Yurasova, Surface N3 (1982) 43 (in Russian); V.A. Eltekov, O.A. Popova and V.E. Yurasova, Radiat. Effects 83 (1984) 39.

[8] C. Kittel, Introduction to Solid State Physics, 4th ed. (Wiley, New York–London–Sydney–Toronto).

[9] V.N. Samoylov, A.H. Phillips and V.A. Eltekov, in: Diagnostics of Surface by Ion Beams, Abstracts of Reps. at All-Union Seminar of Young Scientists, Uzhgorod (1985) p. 191.

[10] D.E. Harrison Jr., W.L. Gay and H.M. Effron, J. Math. Phys. 10 (1969) 1179.

[11] M.V. Kuvakin, A.V. Lusnikov and H.A. Motaweh, Phiz. Tverd. Tela 21 (1979) 2870.

[12] V.E. Yurasova, V.M. Bukhanov and M.V. Kuvakin, Proc. VIIIth Int. Conf. on Ion Phen. in Gases, Beograd (1965) p. 155.

[13] V.E. Yurasova, in: Physics of Ionized Gases, Proc. Invited Lectures at VIIIth Summer School, Dubrovnik (1976), Ljubljana (1976) p. 493.

[14] G.S. Krinchik, L.V. Nikitin, R.G. Bondarenko and R.M. Fedychkin, in: Study and Development of Materials for Thermonuclear Reactors, eds., V.N. Ageev (Nauka, Moscow, 1981) p. 61 (in Russian).

[15] B.A. Kalin, S.N. Korshunov, M.I. Guseva, D.M. Skorov, V.L. Yakushin and I.N. Afrikanov, Surface N12 (1984) 125 (in Russian).